Journal of Coastal Research	SI 39	438 - 387	ICS 2004 (Proccedings)	Brazil	ISSN 0749-0208

Nested Radar Systems for Remote Coastal Observations

P. S. Bell†*, J. J. Williams†, S. Clark‡, B. D. Morris∞ & A. Vila-Concejo∞

†Proudman Oceanographic Laboratory
Joseph Proudman building
6 Brownlow Street
Liverpool, L3 5DA
United Kingdom
psb@pol.ac.uk
jjw@pol.ac.uk

‡ Navtech Electronics Ltd.
Unit 1, The Long Yard
Shefford Woodlands
Hungerford
Berkshire, RG17 7AL
United Kingdom
stevec@nav-tech.com

∞ CIACOMAR/FCMA:
University of Algarve.
Av. 16 de Junho s/n. 8700-311
Olhão
Portugal.
bmorris@ualg.pt
aconcejo@ualg.pt

*Corresponding author

ABSTRACT

BELL, P. S., WILLIAMS, J.J., CLARK, S., MORRIS, B.D. & VILA-CONCEJO A., 2003. Nested Radar Systems for Remote Coastal Observations. Journal of Coastal Research, SI 39 (Proccendigs of the 8th International Coastal Symposium), 438 – 489. Itajaí, SC – Brazil, ISSN 0749-0208

Advances in radar technology now allow the observation of sea surface features at multiple scales, from kilometers, down to metres. In the same manner that nested models are used at different resolutions, nested radars of different frequencies can be used to provide data on sea surface features at various resolutions. A new radar system in the millimeter wave-band has now been demonstrated with a resolution of <1m. This MMW-radar was deployed in a nested configuration with an X-band marine radar from a beach near Faro in Portugal. The results from the two systems show how the MMW-radar can image fine detail surf zone and swash processes to a range of O(200m), while the marine radar provides lower resolution images of O(10m) to longer ranges of O(2km). Data from the two nested radars are shown from a recent deployment on a barrier beach in the Ria Formosa region of the Algarve, Portugal.

The data from these nested radars are analysed to map wavelengths in 2-D and a non-linear bathymetric inversion is used on both sets of data to estimate the bathymetry of the imaged area. Comparisons with in-situ surveys demonstrate the accuracy of this technique.

ADDITIONAL INDEX WORDS: *bathymetry, waves, X-band radar, mm wave radar, depth inversion*

INTRODUCTION

The history of remote bathymetric mapping dates back to the 1940s (Hart & Miskin 1945, Williams 1946), at which time sequences of aerial photographs were analysed by hand to determine wavelengths, directions and velocities for the purpose of mapping enemy beaches using tables of period-wavelength-water depth inversions ready for amphibious landings. Recent developments in remote imaging technologies have brought this technique up to date by providing methods of digitally recording images of the sea surface with high spatial and temporal resolution.

Video techniques have been used both from fixed towers (Holland 2001) and from airborne reconnaissance drones (Dugan 2001) to record optical image sequences of the sea surface. These image sequences can be analysed digitally in a number of ways to extract essentially the same information as that obtained by hand in the 1940s and obtain water depth estimates using depth inversion algorithms (DIAs).

Radar systems also provide a convenient imaging system, allowing large areas of the sea surface to be imaged at relatively shallow grazing angles, negating the requirement of optical techniques for an elevated vantage point. Bell (1999, 2001), Hessner (1999) and Trizna (2001) demonstrated that marine X-band radar could be used with appropriate digital recording systems to provide the required image sequences for bathymetric inversions.

To date, linear wave theory has been the most widely used wave theory to produce a depth inversion algorithm. Trizna (2001) demonstrated that linear theory led to over estimates in water depth in shallow water under high wave conditions and suggested that a non-linear approach would be more appropriate. Holland (2001) used a correction to shallow water linear theory in a DIA designed for water depths of less than 4m and continued to use linear theory in deeper water, considering it to have acceptable accuracy. Work by Bell (2001) also suggested that the non-linear behaviour of waves in very shallow water due to amplitude dispersion was leading to errors in the depth inversions in this region. In the present study a new mm wave (MMW) radar has been used to image breaking waves in this problem region. The MMW radar was deployed in a nested configuration with an X-band radar, allowing the imaging of waves from the swash zone out to water depths of 15m. Depth inversions were carried out based on an equation that approximates the non-linear amplitude dispersion of waves of finite height in shallow water.

EXPERIMENT DESCRIPTION

Two separate radar systems were deployed from the top of a beach near Faro in the Algarve region of Portugal. A marine X-band radar was deployed from a small scaffolding tower at the back of the beach (Figure 1) and a 77GHz MMW radar (Figure 2) was deployed from the top of the beach berm at the same point in the alongshore direction.

The X-band radar has a 1.8m rotating antenna with beam widths of 22^o in the vertical and 1.2^o in the horizontal. The rotation time and hence frame rate of the antenna is nominally 2.4seconds. This type of radar operates by sending out a short 50ns pulse of radar energy, and then 'listening' for the backscattered signals from targets within view of the beam. The time between transmission

Figure 1. The X-Band radar deployed on the beach at Faro during March 2002.

and reception of a signal gives the range of the target and the signal strength gives an idea of the size of the target from its radar cross section. Since the radar pulse travels at the speed of light, high speed recording systems are required to accurately resolve the range of targets. The recording system used for the present study digitises the backscattered radar signals at 20MHz, giving a radial bin length of 7.5m.

The MMW radar operates both at a different frequency and on a different principle to the X-band radar. Instead of transmitting discrete pulses, there is a continuous transmission of a 77 GHz baseband frequency. This frequency is the designated automotive frequency in Europe and the United States, chosen for its low atmospheric absorption (Skolnick 1980). It is also license exempt in most parts of the world, eliminating the need to obtain a license to operate the system. Figure 3 shows how the carrier wave is frequency modulated (FMCW) over 600 MHz in 1mS. The reflected signal is also shown on an expanded time scale. The time between transmission and reception of the radar signal gives a measure of the distance to the reflecting surface as in the X-band radar. However given the limited maximum range, it is not practical to measure such small time intervals. Instead, transmitted and received MMW signals are mixed and the frequency difference extracted, this intermediate frequency being a measure of the target distance.

The MMW radar unit described in this paper employs a 40db lens antenna yielding a beam divergence of approximately 2 degrees. This beam width is spoiled in elevation to approximately

Figure 2. The 77GHz MMW-radar deployed on the beach at Faro during March 2002.

4 degrees to create a fan beam effect. Spreading the beam reduces the signal power returned at a fixed range. For this reason, the maximum radar range in this system is 200 meters at present. The radar images are transferred to a laptop computer via a CAN bus connection, allowing the continuous recording of radar images for hours at a time if necessary.

Recent developments on newer systems by the radar manufacturers have improved hardware design and the signal processing system, providing a range increase to 800m, whilst maintaining the high range resolution. An Ethernet interface has also been added to the radar to acquire the power spectra information at high rate. This makes it possible to acquire several measurements at each azimuth, improving the signal to noise performance of the sensor and allowing smaller waves and effects in the field of view to be extracted.

The X-band radar wave imaging mechanism is based primarily on Bragg scattering from the small capillary ripples on the surface of the gravity waves. There is also some direct specular reflection, particularly from whitecaps and breaking waves which generate a stronger backscatter signal than Bragg scattering alone. This allows regions of breaking waves to be distinguished relatively easily from non-breaking waves. The MMW-radar operates at a considerably higher frequency than the X-band radar and hence the imaging mechanism is also different. It has been observed by the authors that the wave signal seen on these images is based entirely on direct reflection from the foam line or front face of

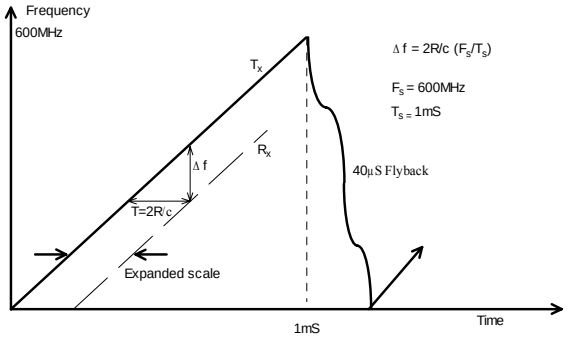

Figure 3. A demonstration of how the range of a target R is proportional to the difference between the transmitted frequency Tx and the received frequency Rx.

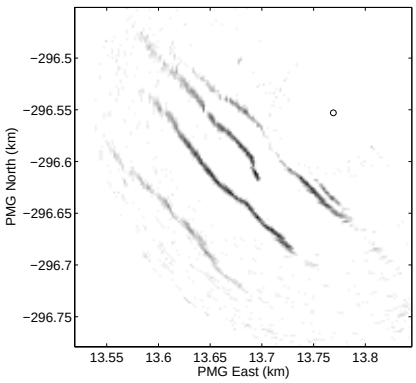

Figure 4. A plot of one image from a sequence of raw MMW-radar data. The 'o' marks the MMW radar location on the beach as shown in Figure 2.

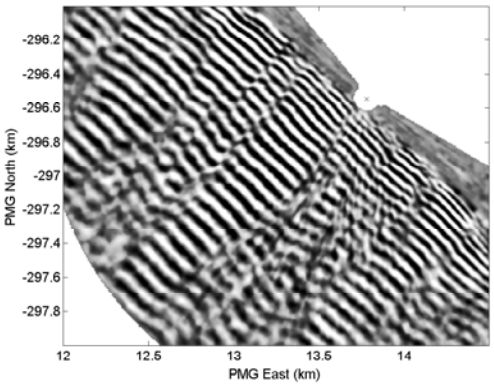

Figure 5. Phase images of 8.9 second waves derived from an X-band radar image sequence. The 'x' marks the deployment location of the radar on the beach.

breaking waves. Hence the wave must be breaking for a wave signal to be seen on the MMW radar. While this may be seen as a restriction in some applications, it has proved to be a strength in others, such as imaging the swash line of beach runup.

Sequences of 128 X-band radar images spanning approximately 5 minutes were recorded digitally every 15 minutes during a storm event on the 4th March 2002. The significant waveheight during the experiment was approximately 2m, determined from the Faro wave buoy in 93 metres of water. The MMW-radar recorded sequences of 512 digital images with a separation of approximately 1 second spanning approximately 9 minutes. The start times of the MMW-radar image sequences were timed to coincide with the start times of the X-band radar sequences so that a direct comparison could be made. An example of a MMW radar image is shown in Figure 4. The dark lines correspond to the foam line of the breaking waves approaching the beach.

A bathymetric survey of subtidal areas was carried out using a boat equipped with a Real Time Kinematic Differential Global Positioning System (RTK DGPS) and an echo sounder on the 21st February 2002, the RTK DGPS allowing the real time tidal correction during the survey. Both the survey and radar locations were referenced to the local Portuguese Melriça Grid (PMG), a recti-linear UTM co-ordinate system. The six cross-shore transects surveyed by the boat were spaced at approximately 20m intervals in the along-shore direction. All transects began close to the shore within the area viewed by both the X-band radar and the MMW-radar and extended approximately 1.5km offshore. A corresponding topographic survey of the beach area, aligned with the offshore transects, was carried out on 4th March 2002. These two surveys were combined and gridded onto one survey that matched the grids used for the radar data.

Records were taken simultaneously from both radars during the rising tide from 11:15am until 15:15. Due to the absence of a nearby tide gauge or in-situ pressure sensor, Poltips software was used to generate 5 minute tidal predictions using harmonic constants determined from data collected during the EU funded INDIA experiment (Williams *et al.* 1999).

DATA ANALYSIS

The analysis of both types of data begins with the conversion from the polar coordinates in which the raw data is recorded to a georeferenced Cartesian grid. For both radars the locations of the transmitters and hence the origins of the polar conversions were determined by RTK DGPS. No slant range to horizontal range correction has been applied in either case as the differences this would make to the final images are a fraction of the final grid pixel sizes in both cases.

A Fourier transform was carried out on each pixel through time in the image sequences to isolate individual wave frequencies. An example of a single frequency image generated by this method for the X-band radar is shown in Figure 5. The corresponding phase image for the MMW radar has been overlaid on that of the X-band radar in Figure 6 illustrating the excellent phase coherence of the waves recorded by the radars. The plots are of the real part of the complex Fourier layer with the grayscale indicating the phase of the waves.

Each frequency layer within the transform was then analysed to map the variations in wavelength across the area viewed by the radars using a discrete 2-D Fourier transform technique that isolates the strongest wave signal in the sub-images. Small subsections of the Fourier layer were used for this analysis, of maximum size 32x32 pixels or 240m square in the case of the X-band radar. In order to make best use of the resolution of the

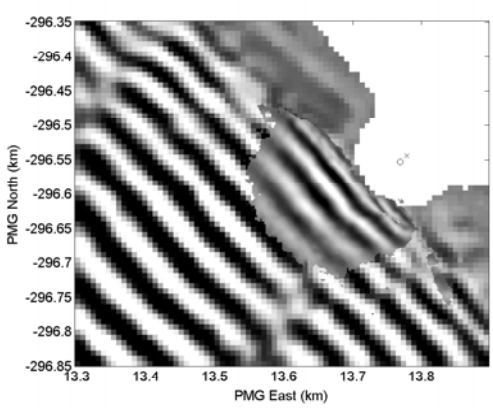

Figure 6. Zoomed phase images of 8.9 second waves, with the x-band radar providing the background image and the higher resolution inlay generated using the MMW radar. The 'x' marks the deployment location of the X-band radar and the 'o' marks the MMW radar location on the beach.

system, this area automatically halved if the number of wavelengths in the sub-image area exceeded 4. The sub-image areas of the MMW-radar were fixed at 16x16 pixels or 32m square. The sizes of these areas were chosen to allow a minimum of one wavelength of the longest period waves in the deepest areas viewed by the respective radars.

The wavelengths calculated from this analysis were then used in a least squares fit to find the water depth at each pixel, calculated both from linear wave theory and from a non-linear wave dispersion equation (Hedges 1976) that approximates the effects of amplitude dispersion of the waves in shallow water:

$$\text{Local wavelength } L = L_0 \tanh k(d+Z) \qquad (1)$$

Where L_0 is the deep water wavelength according to linear wave theory:

$$L_0 = \frac{gT^2}{2\pi} \qquad (2)$$

And Z is a waveheight parameter based on the waveheight H.

Hedges initially suggested a value of $Z = H$ for the waveheight parameter. However, Booij (1981) later suggested that a value of $Z = 0.5H$ would be more appropriate based on experiments carried out by Walker (1976).

This is consistent with the findings of Holland (2001) who found best fits of between $Z = 0.42H_s$ and $Z = 0.48H_s$ in a shallow water simplification of this equation to determine water depths from video image sequences of waves from a number of field sites in water depths of less than 4m. In these instances the offshore significant waveheight H_s was used as the waves observed in the field are spectral in nature and not of a single frequency as might be found in laboratory experiments. A value of $Z = 0.4H_s$ was used in the present analysis and was found to produce excellent results across the full range of depths.

RESULTS

The water depths mapped from this analysis were compared to the survey data with the predicted tidal level added and the results plotted against each other.

Figure 7a shows a cross-shore transect carried out by a survey boat. The water depths determined by using a single record from the X-band radar data are shown as 'x' symbols and the water depths determined by using a single record of the MMW-radar data are shown as 'o' symbols. The region closest to the shore is magnified in Figure 7b to emphasize the detail in that area. In waters more than 150m from the shore the X-band radar depth estimates show very good correlation with those of the survey.

In waters nearer the shore, edge effects and the finite size of the analysis area start to degrade the depth estimates. However, the depth estimates made using the smaller analysis areas made possible by the higher resolution MMW radar show that the algorithms used are still valid within this region. The depth estimates made using the MMW radar are all within 0.5m of the survey, and usually considerably better.

A further illustration of this is shown in Figure 8, in which the radar estimated water depths are compared to those of the survey. The diagonal line denotes the 'ideal' result of the radar determined water depths matching those of the survey. The averaging of a number of such results through a tidal cycle by subtracting the tidal level and working to chart datum serves to reduce the scatter

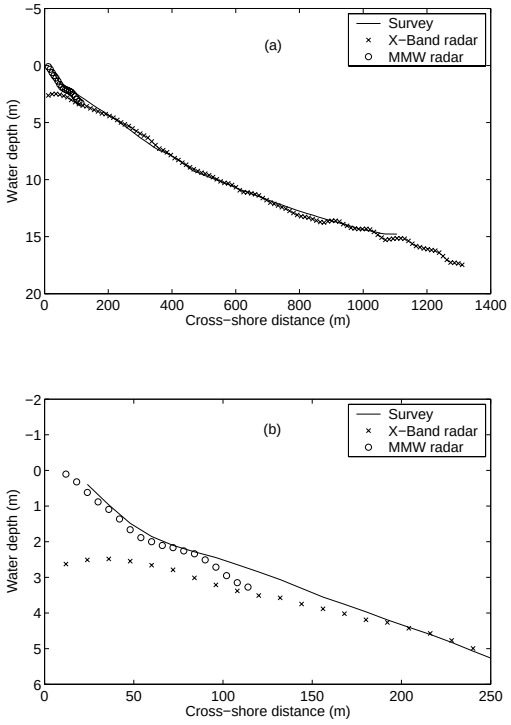

Figure 7. A cross-shore transect surveyed by boat overlaid with depths determined using data from a single record of the X-band radar and MMW radar.

and increase accuracy in the resulting bathymetric maps, although examples are not shown here.

DISCUSSION

It has been demonstrated that a nested configuration of radars of different resolutions and ranges can provide the data required for estimating the bathymetry of an area using a depth inversion

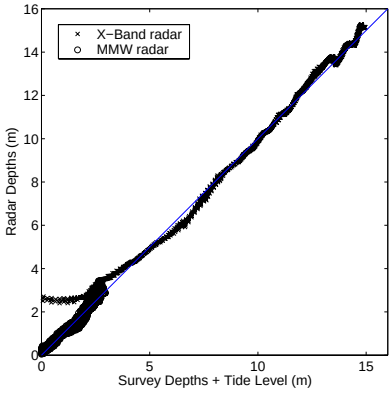

Figure 8. A scatter plot of radar derived water depth compared to those determined by a survey boat.

algorithms. Hedges' equation approximating the non-linear effects of amplitude dispersion is very effective at bringing the radar derived water depths into close agreement with those of the survey, right up to the shoreline. This is an interesting result as a degree of wave setup might be expected that close to the shore under in such storm conditions, increasing the mean water level by an amount of the order of tens of cms. The waveheight correction to linear theory that the equation applies is unrealistically large in the shallowest depths, with the water depths implied by the analysis being physically unable to support this height of wave. However, it would appear that this overly large correction is almost exactly cancelling out the probable existence of an elevated mean water level due to wave setup.

This was investigated by adding a depth limited breaking term to the analysis which limited the waveheight in the shallowest depths to a more realistic level of half the water depth. This consistently showed an elevated mean water level of the size that might be expected from wave setup. Unfortunately there were no in-situ pressure sensors with which to confirm these findings in the present experiment. It is hoped that this can be investigated in more depth in future experiments.

There are several possibly sources of error that should be considered in the present study. The mean water depth used is based on a tidal prediction and as such does not include set-up or set-down caused by meteorological effects. This is considered a minor source of error as previous experience with the field site suggests that residual water levels attributable to these effects are unlikely to be larger than 15-20cm.

A further possible source of error exists in the surveyed water depths due to the time gap of several days between the boat survey and the radar measurements. This could introduce small errors in shallower water depths. Considering the storm conditions involved it is even possible that the bathymetry of the region closest to the shore could change slightly within the time taken to conduct the experiment.

The wave height measurements were obtained by reading the waveheight from the graphs of wave buoy data displayed on the website of the Instituto Hidrografico in Portugal (www.hidrografico.pt) from which readings can generally be read to an accuracy of +/-0.25m or better.

The influence of currents, both tidal and wave induced, are also a potential source of variability in the water depth estimates. Such currents would cause a Doppler shift to the waves, making the derived water depths larger if the current is in the direction of wave motion, or smaller if the current is in opposition to the waves. Rip currents in particular could cause localized errors in the derived water depths due to their strength and the fact that they would tend to directly oppose waves approaching the beach. Tidal currents are not thought to be of such importance, at least on a straight beach such as this as they will tend to be perpendicular to the wave direction and hence have little effect on the waves.

Further experiments involving nested radar systems are in preparation. Proudman Oceanographic Laboratory are currently installing a 16MHz WERA HF radar to provide current and wave data in the Liverpool Bay area of the Irish Sea as part of the POL Coastal Observatory. Within this area, an X-band radar has been installed on a remote island in the Dee Estuary, an area with an extensive system of sand banks that are known to be in a constant state of evolution, helped by a spring tidal range in excess of 10m. The deployment of both systems is planned to be of at least 5 years duration, presenting the possibility of monitoring the evolution of the system of sand banks remotely using bathymetric inversions of X-band radar data.

REFERENCES

BELL, P.S., 1999, "Shallow water bathymetry derived from an analysis of X-band marine radar images of waves". *Coastal Engineering* (37), 03-4, pp.513-527.

BELL, P.S., 2001. "Determination of bathymetry using marine radar images of waves". Proceedings of the *4th International Symposium on Ocean Wave Measurement and Analysis*, San Francisco, California, Vol. 1, 251-257.

BOOIJ, N., 1981, "Gravity waves on water with non-uniform depth and current". *Rep. No.81-1*, Dept. Civ. Eng., Delft university of Technology.

DUGAN, J.P., PIOTROWSKI, C.C. and WILLIAMS, J.Z., 2001. "Water depth and surface current retrievals from airborne optical measurements of surface gravity wave dispersion". *J. Geophysical Research*, Vol. 106, No. C8, pp 16903-16915.

HESSNER, K., REICHERT, K. and ROSENTHAL, W., 1999. Mapping of sea bottom topography in shallow seas by using a nautical radar". *2nd Symposium on Operationalization of Remote Sensing*, ITC, Enschede, Netherlands, 16-20th August 1999.

HART, C.A. and MISKIN, E.A., 1945, "Developments in the method of determination of beach gradients by wave velocities". *Air survey research paper no. 15, Directorate of Military Survey, UK War Office.*

HEDGES, T.S., 1976, "An empirical modification to linear wave theory". *Proc. Inst. Civ. Eng.*, 61, 575-579.

HOLLAND, T.K., 2001, "Application of the linear dispersion relation with respect to depth inversion and remotely sensed imagery". *IEEE Trans. Geos. & Remote Sensing*, 39, 2060-2072.

SKOLNIK, M.I., 1980, "Introduction to Radar Systems Second edition". *McGraw Hill*.

TRIZNA, D.B., 2001, "Errors in bathymetric retrievals using linear dispersion in 3-D FFT analysis of marine radar ocean wave imagery". *IEEE Transactions on Geoscience and Remote Sensing*, Vol. 39, No.11, 2465-2469.

WALKER, J.R., 1976, "Refraction of finite-height and breaking waves". Proc. *15th international conference on Coastal Engineering*, Honolulu, Hawaii, Published by A.S.C.E. New York 1977.

WILLIAMS J. J., ARENS B., AUBREY D., BELL P., BIZZARO A., COLLINS M., DAVIDSON M., DIAS J., FERREIRA O., HERON M., HOWA H., HUGHES Z., HUNTLEY D., JONES M. T., O'CONNOR B., PAN S., SARMENTO A., SEABRA-SANTOS F., SHAYLER S., SMITH J., VOULGARIS G. (1999). "Inlet Dynamics Initiative: Algarve (INDIA)". Proceedings *Coastal Sediments'99*, ASCE, Long Island, New York, USA, 16pp.

WILLIAMS, W.W., 1946, "The determination of gradients on enemy-held beaches". *Geogr. J.* XIC, 76-93.

ACKNOWLEDGEMENTS

The authors would like to thank the Parque Natural da Ria Formosa for their kind permissions to carry out the fieldwork. The authors would also like to thank the Portuguese FCT funded CROP project (PDCTM/MAR/15265/99) for supplying the bathymetry/topography data and for funding A. Vila-Concejo.

Many thanks to Dr David Blackman for carrying out the tidal analysis and supplying the tidal constituents for the beach at Faro.

This work has been carried out as a component of a part-time PhD by P.S. Bell in association with the University College of North Wales, Bangor.